Osmotically driven shape-dependent colloidal separations

T. G. Mason

Corporate Strategic Research, ExxonMobil Research and Engineering Co., Route 22 East, Annandale, New Jersey 08801
(Received 28 December 1999; revised manuscript received 11 October 2002; published 30 December 2002)

The thermally induced motion of nanometer-sized surfactant micelles in water is used to create strong attractive forces between micron-sized disks of wax in a mixed aqueous dispersion of microdisks and microspheres. The short-ranged attractive force due to the depletion of micelles from between the microdisks is much stronger than that between two microspheres of similar size, and is largest when the disks approach face to face, so columns of microdisks form. These columns cream, whereas the spheres remain dispersed, providing a means for shape-dependent colloidal separations driven by an applied micellar osmotic pressure.

Complex dispersions of colloidal particles having different shapes and sizes in a suspending fluid are widely encountered in physical and biological contexts [1,2]; examples range from blood [3–5] to liquid crystal dispersions [6]. Isolating similarly shaped particles in a complex dispersion is an important problem. For years, biomedical researchers have isolated viruses and proteins from the contents of ruptured cells by adding polymers to selectively aggregate and then separate the desired component [7–10]. However, no clear quantitative study of how shape selectivity arises from depletion attractions caused by the polymers has been made. A rich variety of entropically driven microphase transitions has been found in two-component mixtures of microscopic rods and spheres having similar dimensions [11]. Three-component mixtures of differently shaped and differently sized colloids are likely to yield an even greater variety of structures.

Here, we show that micron-sized spheres and disks in a complex dispersion can be separated by adding a third particulate component, nanospherical colloids, to control shape-selective aggregation. We study the aggregation of micron-sized disks and spheres of 1-eicosene wax in a dilute aqueous dispersion [12] induced by nanometer-sized spherical micelles of sodium dodecylsulfate (SDS) surfactant [13]. By controlling the micelle concentration, we create entropic short-ranged depletion attractions [14–18] that cause the preferential aggregation of microdisks into columns, and subsequently bundles, but leave the microspheres unaggregated. We show that the depletion attraction between two disks oriented face to face is much larger than the sphere-disk [19] and sphere-sphere [14,16] attractions. By analogy to fractionated crystallization [20], the aggregated disks can be repeatedly separated from the unaggregated spheres by gravitational creaming, yielding a shape-specific colloidal purification method.

Microspheres in solution aggregate when much smaller nanospheres are introduced at a sufficiently high concentration to create a strong depletion attraction [14,16]. When two microspheres approach closely, a volume that excludes the smaller spheres is formed, and the nonuniform effective pressure of the smaller spheres over the surfaces of the larger spheres creates a net attractive force. This short-ranged, entropic depletion attraction depends on the concentration of smaller spheres and on the size ratio of large to small spheres. Fractionated crystallization exploits this size depen-

dence to split a dispersion of broadly polydisperse microspheres into several dispersions of uniformly sized microspheres by repeatedly aggregating and separating large from small microspheres using nanoscale surfactant micelles [20].

We make the wax dispersion by heating and shear mixing liquid 1-eicosene into a highly concentrated aqueous solution of SDS. In addition to forming micelles, the SDS coats the surfaces of the liquid wax droplets and provides a screened electrostatic repulsion that inhibits coalescence and irreversible aggregation. The suspension is diluted and cooled to room temperature $T = 23\,°C$ below the 1-eicosene freezing temperature $T_f \approx 26\,°C$ [12]. After many weeks at an SDS concentration of $C = 40$ mM, we dilute 50 μl of the aggregated and creamed wax particles in 1 ml of distilled water. Optical differential interference contrast microscopy of the dilute solution reveals particles consisting of about 95% spheres having radius $a_s = 0.5\,\mu$m and radial root-mean-square polydispersity $P_a \approx 0.25$, and 5% disks (short cylinders) having average radius $a_d = 0.5\,\mu$m (similar polydispersity) with an average aspect ratio of thickness to diameter of $\varepsilon = 0.2$. The disks are optically birefringent, consistent with the alignment of the 1-eicosene molecular axes along the disk's symmetry axis.

We explore how the micelle concentration affects the particle interactions by microscopically observing the suspension for particle volume fractions near $\phi \approx 10^{-3}$, 1 h after setting C. For C below the critical micelle concentration of SDS, $C^* = 8$ mM, we observe that neither the spheres nor the disks aggregate. However, for $C > C^*$, we find that the disks aggregate over a wide range of C, whereas spheres having similar radii remain dispersed. The aggregates are primarily long rodlike columns of many disks stacked face to face at $C = 20$ mM [Figs. 1(a) and 1(b)]. These columns are not perfectly rigid, since entropic excitations lead to noticeable transverse displacements of the disks within the column relative to the column's axis. At larger disk volume fractions, we observe that columns are attracted to each other and form bundles [Fig. 1(c)]. We also find that disks with very large radii may serve as baseplates for several disks of smaller radii, resulting in flat disordered stacks. For $C > 30$ mM, not only do the disks aggregate, but the spheres aggregate with other spheres. The aggregation is reversible, since the aggregates break up and the disks redisperse when C is lowered below C^*. These observations of disk and sphere aggregation are summarized in Fig. 2(a).

　　　　　　　　　　　　　　　　　　 66 060402-1
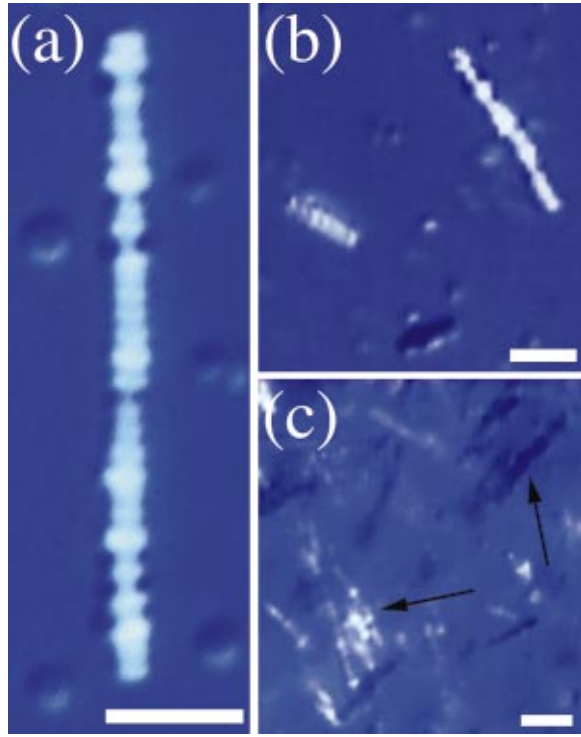
FIG. 1. (Color) Optical micrographs of (a) a rodlike columnar aggregate of 1-eicosene colloidal disks and unaggregated spheres in an aqueous micellar SDS solution at an SDS concentration $C = 20$ mM, (b) columnar aggregates and unaggregated spheres in a dilute solution at a total volume fraction $\phi \approx 10^{-3}$ and $C = 20$ mM, (c) columnar aggregates bundle at larger $\phi \approx 10^{-2}$ (arrows). Scale bars are 3 μm.

In order to understand the aggregation, we consider the energy U_c due to the depletion of micelles between two differently shaped particles at contact. This energy is the product of the excluded volume of micelles between the particles, V_e, with the micellar osmotic pressure $\Pi_m \equiv C_m N_0 k_B T$, where k_B is Boltzmann's constant, N_0 is Avagadro's number, $C_m = (C - C^*)/\nu$ is the micelle molar concentration, and $\nu \approx 70$ is the number of SDS molecules needed to form a micelle [13]. Below C^*, the observed lack of aggregation in Fig. 2(a) is consistent with the absence of micelles. Above C^*, U_c can be estimated using a simple geometrical determination of V_e.

For two spheres, depicted in Fig. 3(a), the excluded volume can be approximated by a cylinder of radius $(2a_s a_m)^{1/2}$ and length $2a_m$. This yields $V_e = 4\pi a_m^2 a_s$ and

$$U_c^s = -4\pi a_m{}^2 a_s \Pi_m, \qquad (1)$$

where $a_m \approx 20$ Å is the micelle radius. This result agrees with an exact calculation of the contact energy [16]. Using $a_s = 0.5$ μm, we plot $|U_c^s|$ in Fig. 2(b). The observed aggregation of spheres for $C \geq 30$ mM establishes $|U_c| \geq 4k_B T$ as an empirical aggregation criterion. The contact energy between a sphere and a disk face [19,21] is simply $2U_c^s$.

For two identical disks with $\varepsilon \ll 1$, $|U_c|$ is maximal when they approach face to face, shown in Fig. 3(b). The excluded
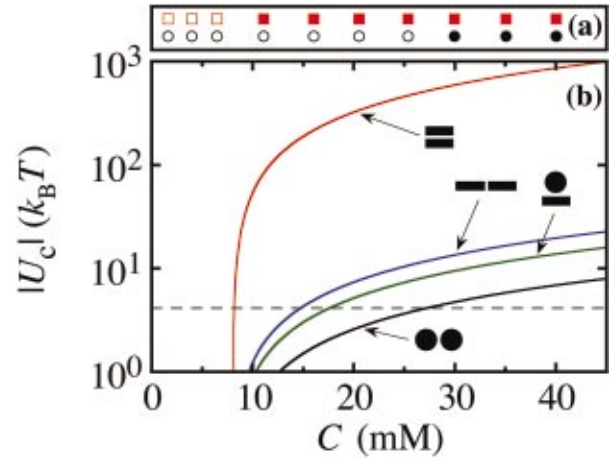
FIG. 2. (Color) (a) Microscopic observations reveal aggregation (solid symbols) or no aggregation (open symbols) of disks (squares) or spheres (circles) as a function of SDS concentration C. (b) The contact energy $|U_c(C)|$ for sphere-sphere, sphere-disk, disk-disk (side-side), and disk-disk (face-face) depletion interactions (solid lines from bottom to top) calculated using radii $a_s = a_d = 0.5$ μm and a length to diameter aspect ratio $\varepsilon = 0.2$. Aggregation occurs for $|U_c(C)| > 4k_B T$ (dashed line); only disks aggregate for 10 mM $< C < 20$ mM.

volume can be estimated by the product of the disk's facial area with the micelle diameter, yielding $V_e = (\pi a_d{}^2)(2a_m)$ and

$$U_c^d = -2\pi a_m a_d{}^2 \Pi_m. \qquad (2)$$

This contact energy does not depend on ε and is much stronger than either the sphere-sphere or disk-sphere interactions $|U_c|$ for identical radii $a_d = a_s = 0.5$ μm at the same C [Fig. 2(b)]. If the two interacting disks have different radii, then a_d in Eq. (2) is the radius of the smaller disk. The criterion of $|U_c| \geq 4k_B T$ implies that disks will aggregate for C just above C^*.

Two disks may also approach side by side with an edge overlap distance of z, as shown in Fig. 3(c). Here, V_e can be estimated by a rectangular parallelepiped having length z, width $(2a_m a_d)^{1/2}$, and thickness $2a_m$; so the contact energy is

$$U_c^r = -2^{5/2} z a_m{}^{3/2} a_d{}^{1/2} \Pi_m. \qquad (3)$$

Since the maximum excluded volume will be attained at full overlap ($z = 2\varepsilon a_d$), U_c^r is proportional to the aspect ratio. For coinlike disks with $\varepsilon = 0.2$ and $a_d = 0.5$ μm, Eq. (3) is much smaller than Eq. (2) at the same C, as shown in Fig. 2(b), implying that disks would prefer to aggregate face to face into columns. As the columns grow longer, z could become large enough that $|U_c^r| \geq 4k_B T$, so columns could aggregate side by side into bundles.

The stability of individual columnar stacks against thermal transverse fluctuations can be explained by considering the depletion energy between two disks when their axes are separated by a transverse displacement $2r$. The transverse contact potential energy $U_\perp$ is given by the product of U_c for
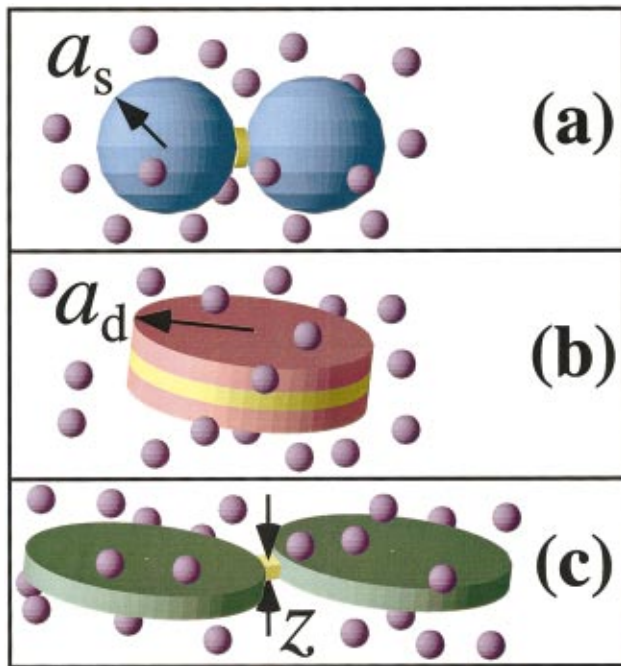
FIG. 3. (Color) Schematic representations of the excluded volumes (yellow) between (a) two spheres of radius a_s; (b) two disks of radius a_d, oriented face-to-face; and (c) two disks oriented side by side with an edge overlap distance z. The small purple spheres represent micelles (not to scale).

FIG. 4. Shape-selective separation of colloidal disks from spheres. (a) The SDS concentration is raised above the C^*, so that SDS micelles (small dots) drive columnar aggregation of disks but not spheres. To the right is shown a schematic of the radial size distribution of the spheres (solid line) and disks (dashed line). (b) The large columnar aggregates cream under gravity much faster than the unaggregated spheres, thereby concentrating the disks in the cream.

perfectly aligned disks with a dimensionless factor representing the overlap area normalized by the disk's facial area. This results in a steep anharmonic potential well about $r = 0$, which corresponds to a transverse restoring force $f_\perp(r) = -[4U_c^d/(\pi a_d)]\sqrt{1-(r/a_d)^2}$, opposing any misalignment of the disks' axes. For $C = 25$ mM and $r/a_d \ll 1$, the restoring force is nearly independent of r and is quite strong, yielding $|f_\perp| \approx 1 k_B T$/nanometer, so thermal excitations of identical micron-sized disks in a column should yield only nanometer-scale transverse displacements. By contrast, for two disks having different radii, the contact energy is independent of the axial alignment until the small disk encounters a strong restoring force at the edge of a large disk and is effectively reflected [19]. Many disks having different radii in a column will exhibit coupled diffusion with reflective boundary conditions. Thus, the micron-scale variation in the disk radii leads to micron-scale transverse displacements and floppy columns with slow modes of vibration, as we observe.

The large disk-disk attractive energy relative to the disk-sphere and sphere-sphere energies suggests that a mixed dispersion of similar-sized disks and spheres can be separated by raising the micelle concentration into the regime where disks aggregate but spheres do not. This is shown schematically in Fig. 4(a). The optimal C maximizes $|U_c^d|$ without introducing significant disk-sphere aggregation, so we set $C \approx 15$ to 20 mM. The density difference between the wax and the water leads to gravity-driven creaming of the large columnar aggregates, whereas the spheres remain dispersed in the solution below, as shown in Fig. 4(b). By skimming off

the cream, redispersing it to $\phi \approx 10^{-2}$ at $C < C^*$ and repeating the process several times to get rid of contaminating spheres left in the cream, we obtain a purified dispersion of disks. Six separation steps are needed to obtain a ratio of 95% disks to only 5% spheres. These purified colloidal disks may serve as a model system for studying the phase behavior of discotic liquid crystals [6].

The columnar discotic aggregates appear to have unique features. They differ greatly from the "house of cards" [22] and random [23] structures of gels of inorganic clay disks that have negatively charged faces and positively charged rims. Although the columnar aggregates of disks resemble the stacked-coin structures of red blood cells (RBCs), known as rouleaux [3,4], which form when polymers are added to blood, there are important differences between the two systems. Since normal RBCs have dimpled faces and, for the purpose of calculating face-face depletion interactions, resemble toroids, we would expect the largest excluded volume to resemble an annular disk, and the contact energy of the toroid, U_c^t, would be less than that for perfectly flat disks, $U_c^t = -2^{5/2}\pi a_t a_m^{3/2} a_c^{1/2}\Pi_m$, where a_c is the radius of the toroid's circular cross section and a_t is the toroidal radius given by the distance from its symmetry axis to the center of the circular cross section. Thus, a significantly smaller concentration of micelles is sufficient to induce the aggregation of disks into columns as compared to similarly-sized RBCs.

The second major difference lies in the entropically driven vibrational modes of the columnar aggregates. The transverse fluctuations of RBCs in rouleaux would be much smaller in amplitude and of a higher frequency than the slow floppy modes of the column of polydisperse disks. Finally, branching or ''T structures'' would be much more prominent for RBCs than for disks because the depletion potential for the edge of a RBC interacting with the dimple of another RBC in a T configuration is of the same order of magnitude as U_c^t. By contrast, for flat disks, the depletion potential for the T configuration is much smaller than U_c^d. This approach for RBCs may also serve as a basis for understanding stacked annular disk aggregates of tobacco mosaic virus protein [24].

To quantify the degree of separation that one may expect between colloids of a different shape but similar volume, we introduce a dimensionless shape-dependent separation factor S. Consider the maximum excluded volumes for all possible orientations between unique pairs of colloids relative to the sphere-sphere excluded volume. We define the separation factor to be the ratio of the largest pair excluded volume to the smallest pair excluded volume. For example, for spheres and disks having identical volume, the largest pair excluded volume is U_c^d and the smallest is U_c^d, so $S = (2\varepsilon)^{1/3}(a_d/a_m)$. For $S \approx 1$, there will be little shape specificity in a single separation step and it must be repeated many times in order to achieve a significant purity. However, for $S \gg 1$, it will be possible to efficiently separate at least one pair of components in the mixture with relatively few steps, as we have observed with disks and spheres.

The method of shape-selective colloidal separation we have demonstrated with spheres, disks, and micelles may be applicable to a broad class of mixtures of isotropic and anisotropic particles. By exploiting the shape-dependent strength of the depletion attraction between large colloids, such as spheres, disks, facetted microcrystallites, and rods, through the controlled concentration of a much smaller colloid, such as micelles or polymers, preferential aggregation of specific larger colloids may be induced. It would be interesting to examine the separation factors for biological colloids such as cells, viruses, organelles, or proteins found in dispersed tissue and to compare these with the efficiency of separations found experimentally.

The wax microdisks that we have purified through shape-selective separation have been trapped, aligned, and spun optically using laser tweezers [25] and have also been used to study rotational Brownian motion in viscoelastic liquids [26]. Based on the work presented in this Rapid Communication, we anticipate that one can lithographically engineer lock and key building blocks having different excluded volumes that self-assemble in a controlled sequence into a larger superstructure as the osmotic pressure is increased.

[1] W. B. Russel, D. A. Saville, and W. R. Schowalter, *Colloidal Dispersions* (Cambridge University Press, Cambridge, England, 1989).

[2] B. Alberts, D. Bray, J. Lewis, M. Raff, and K. Roberts, *Molecular Biology of the Cell* (Garland, New York, 1994).

[3] R. W. Samsel and A. S. Perelson, Biophys. J. **37**, 493 (1982).

[4] A. S. Perelson and F. W. Wiegel, Biophys. J. **37**, 515 (1982).

[5] K.-M. Jan and S. Chien, Biorheology **16**, 137 (1979).

[6] P. G. deGennes and J. Prost, *The Physics of Liquid Crystals* (Oxford University Press, Oxford, 1993).

[7] S. S. Cohen, J. Biol. Chem. **144**, 353 (1942).

[8] T. T. Herbert, Phytopathology **53**, 362 (1963).

[9] R. Leberman, Virology **30**, 341 (1966).

[10] K. R. Yamamoto, B. M. Alberts, R. Benzinger, L. Lawhorne, and G. Treiber, Virology **40**, 734 (1970).

[11] M. Adams, Z. Dogic, S. L. Keller, and S. Fraden, Nature (London) **393**, 349 (1998).

[12] H. Gang, O. Gang, H. H. Shao, X. Z. Wu, and I. Patel, J. Phys. Chem. B **102**, 2754 (1998).

[13] B. Cabane, R. Duplessix, and T. Zemb, J. Phys. (Paris) **46**, 2161 (1985).

[14] S. Asakura and F. Oosawa, J. Chem. Phys. **22**, 1255 (1954).

[15] L. Onsager, Ann. N.Y. Acad. Sci. **51**, 627 (1949).

[16] A. Vrij, Pure Appl. Chem. **48**, 471 (1976).

[17] P. A. J. Forsyth, S. Marcelja, D. J. Mitchell, and B. W. Niham, Adv. Colloid Interface Sci. **9**, 37 (1978).

[18] H. N. W. Lekkerkerker and A. Stroobants, Nuovo Cimento Soc. Ital. Fis., C **16**, 949 (1994).

[19] A. D. Dinsmore, A. G. Yodh, and D. J. Pine, Nature (London) **383**, 239 (1996).

[20] J. Bibette, D. Roux, and F. Nallet, Phys. Rev. Lett. **65**, 2470 (1990).

[21] J. N. Israelachvili, *Intermolecular and Surface Forces* (Academic Press, London, 1992).

[22] M. Dijikstra, J. P. Hansen, and P. A. Madden, Phys. Rev. Lett. **75**, 2236 (1995).

[23] M. Kroon, W. L. Vos, and G. H. Wegdam, Phys. Rev. E **57**, 1962 (1998).

[24] R. Díaz-Avalos and D. L. D. Caspar, Biophys. J. **74**, 595 (1998).

[25] Z. Cheng, P. M. Chaiking, and T. G. Mason, Phys. Rev. Lett. **89**, 108 303 (2002).

[26] Z. Cheng and T. G. Mason, Phys. Rev. Lett. (to be published).